Coupled iron-microbial catalysis for CO2 hydrogenation with multispecies microbial communities

Elise Blanchet, Zoï Vahlas, Luc Etcheverry, Yan Rafrafi, Benjamin Erable, Marie-Line Délia, Alain Bergel

Coupled iron-microbial catalysis for CO_2 hydrogenation with multispecies microbial communities

Elise Blanchet, Zoï Vahlas, Luc Etcheverry, Yan Rafrafi, Benjamin Erable, Marie-Line Délia, and Alain Bergel*

Laboratoire de Génie Chimique, CNRS, Université de Toulouse (INPT), 4 allée Emile Monso, 31432 Toulouse, France.

** Corresponding author: alain.bergel@ensiacet.fr*

Abstract. The hydrogenation of carbon dioxide offers a large range of possible reactions for converting hydrogen to chemical compounds that can be easily stored, transported and used as fuels or platform molecules. In this study, CO_2 hydrogenation was biocatalysed by multispecies microbial communities to produce formate, butyrate and acetate. A hybrid metal/microbial catalysis was pointed out in the presence of iron. Addition of $FeCl_3$ 10 mM increased the production of acetate by 265 % and butyrate by 73 %, to 5.26 and 14.19 g/L, respectively. A stable acetate production rate of 830 mg/L/d was thus sustained for more than 20 days. The presence of iron promoted the selection of Firmicutes and the best performances were linked to the growth of a restricted number of dominant species of two genera: *Clostridium* and *Megasphaera*. Various possible catalysis mechanisms are discussed and guidelines are proposed for further development and scale-up of the process.

Keywords: biocatalysis; gas-liquid; green chemistry; sustainable chemistry; environmental inoculum; electron transfer.

1. Introduction

The production of electricity from renewable sources such as hydropower, sunlight, wind, marine streams, tides and biomass holds great promise [1] but these sources show great variability, which will subject the electricity grid to large fluctuations. The electrical energy produced during the favourable periods must consequently be stored. Producing hydrogen by water electrolysis offers an attractive way to store electrical energy in chemical form and thus mitigate the fluctuations of the sources. However, storing large quantities of hydrogen remains a technological challenge: in gas form, it is explosive and highly diffusive [2,3] and its conversion to liquid form consumes an amount of energy that severely impacts the final energy balance [1]. A transformation of hydrogen into easier-to-handle chemical compounds is consequently highly desirable.

The combination of hydrogen with carbon dioxide offers the possibility to convert hydrogen into various energy carriers and microorganisms have revealed very interesting catalytic possibilities for these reactions. Microbial catalysis of CO_2 hydrogenation has been shown to lead to the production of methane [4-8], formate, acetate, ethanol, butyrate, 2.3-butanediol, and butanol [9-11], i.e. compounds that can be used as energy carriers and also as feedstock for chemical industries.

The capacity of *E. coli* to produce formate from CO_2 and H_2 was identified in the 1930's [12]. Catalysis of this reversible reaction by *Alcaligenes eutrophus* (renamed *Cupriavidus necator*) was proposed as a hydrogen storage system as early as 1982 [13]. Since then, other microorganisms have shown the capacity to catalyse the hydrogenation of CO_2 to formate [14,15].

Hydrogenation of CO_2 to acetate by acetogenic microorganisms was first reported in 1932 [16]. Acetogenic organisms such as *Clostridium autoethanogenum*, *Clostridium ljungdahlii*, and *Clostridium ragsdalei* can also produce ethanol [11]. In some cases butyrate, 2.3-butanediol, or butanol can be synthesized in addition to acetate [10].

To date, the microbial catalysis of CO_2 hydrogenation has mainly been performed with pure cultures. Surprisingly, the use of multispecies inocula remains rare [17,18]. Multispecies cultures have so far been used almost exclusively for the production of methane [4-7]. The biogas produced by anaerobic digesters contains significant levels of CO_2 as a by-product and biogas can be upgraded by converting this CO_2 to CH_4 with hydrogen. Outside the field of methane production, very few studies

have described the use of multispecies inocula for CO_2 hydrogenation. To the best of our knowledge, only two recent works have implemented multispecies inocula and showed their capacity to catalyse the conversion of CO_2 and H_2: to a mixture of acetate, butyrate, caproate and caprylate in one case [17] and to formate or acetate in the other [18].

From a technological standpoint, if the objective is to scale up to large sized commercial reactors, environmental inocula present the great advantage, over pure cultures, of not requiring sterile conditions [19]. Microbial consortia coming from environmental inocula should consequently be sources of robust microbial CO_2 hydrogenation catalysts that can operate without the drastic constraints related to pure cultures.

The present study describes a new way to catalyse the microbial hydrogenation of CO_2 by using multispecies inocula obtained from salt marsh sediments and sludge from a wastewater treatment plant. The presence of iron in solution was discovered to considerably enhance the production of formate, acetate and butyrate. To the best of our knowledge, this was the first demonstration of such a hybrid catalysis that combines metal and microorganisms for CO_2 hydrogenation. This finding greatly increased the efficiency of the microbial catalysis and is thus an essential step in implementing environmental microbial consortia in large-sized industrial CO_2 hydrogenation processes. It provides bioengineers with a new method of efficient CO_2 hydrogenation, as an essential building brick in the construction of the future hydrogen economy.

2. Materials and methods

2.1 Solutions and inocula

The minimal medium used for most experiments was the “2260 Freshwater” ATCC medium, omitting electron acceptor and donor [20]. It contained KCl (0.1 g/L), NaH_2PO_4 (0.6 g/L), NH_4Cl (1.5 g/L), $NaHCO_3$ (2.5 g/L), trace minerals (10 mL/L, ATCC MD-TMS) and vitamins (10 mL/L, ATCC MD-VS). This medium was inoculated with biological sludge collected from a water treatment plant (Suez Environnement, Evry, France) at 3.3% v/v (7 mL sludge for 210 mL final volume), except when another ratio is indicated (run #2). Before being used to inoculate the solution, the sludge was exposed to an H_2-N_2:CO_2 (80:20%) atmosphere for 5 days at 30°C to favour the development of

homoacetogenic bacteria. After the 5-day acclimation, the presence of acetic acid at 1980 mg/L and butyric acid at 23 mg/L was detected by HPLC.

A high-salinity medium was also used, which was the minimal medium with the addition of NaCl (45 g/L), $MgCl_2$ (0.1 g/L) and $CaCl_2$ (0.01 g/L). This medium was inoculated with sediments (10% v/v) collected from a salt marsh of the Mediterranean Sea (Gruissan, France). The presence of lactic acid (370 mg/L), formic acid (91 mg/L) and butyric acid (83 mg/L) were detected by HPLC.

2.2 Experimental set-up

Gas scrubber bottles were used as gas/liquid contactors (GLC) as schematized in Figure 1. They were filled with 210 mL of solution including the inoculum. Solution sampling was carried out through a connection hermetically sealed with a septum seal. In the initial version of the GLC, gas feeding was achieved with a simple pipe, which delivered gas bubbles around 3 mm in diameter. In the second GLC version, in order to improve gas/liquid transfer, the gas was provided through a porous tube about 5 cm long with a diffuser at the end that delivered fine bubbles. In some cases, a mixture of N_2:CO_2 was used instead of pure CO_2 in order to ensure a low CO_2 flow rate. In all cases, the flow rates indicated in the text and figure legends give the inlet quantity of pure CO_2.

Some GLC were packed with a fixed bed made of 316L stainless steel grids (0.6 mm diameter wires, 5 mm mesh, Toul'Inox, France) with a total geometric surface area of 320 cm^2, or another surface area where indicated, or with commercial steel wool (grade 000, Fe 93%, C 6.1%, Mn 0.8%), which was positioned in roughly half of the CGL volume. When indicated, the methanogenic inhibitor sodium 2-bromoethanesulfonate (BES) was added. Reactors were maintained at 30°C in a water bath. Initially, the pH values ranged from 7.1 to 8.0 depending on the inoculum and the inoculum ratio.

Hydrogen conversion yields were calculated as:

$$\frac{R_{product}}{Q_{H2}} \text{ n } V_m \qquad (1)$$

where $R_{product}$ is the molar production rate of the product (mol/d), Q_{H2} is the hydrogen flow rate (L/d), n is the number of moles of hydrogen required to obtain 1 mole of product (n = 4 for acetate production) and V_m is the molar volume of perfect gas (22.4 L/mol).

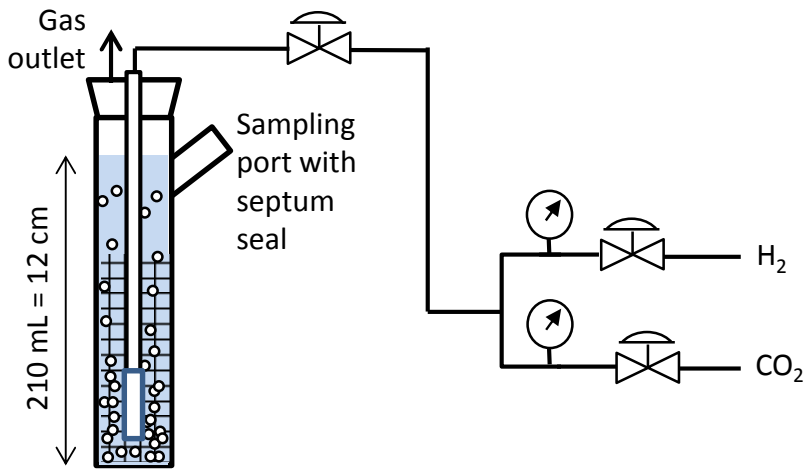

Fig.1. Scheme of the gas/liquid contactors (GLC) and experimental set-up

2.3 Analyses

Samples were collected every day or every two days, filtered at 0.2 µm and analysed for organic acids, sugar and ethanol by HPLC (Thermo Scientific, France) using a Rezex ROA-Organic acid H+ (8%), 250*4.6 mm phase-reverse column (Phenomenex, France) thermostated at 30°C and associated with a refractive index detector in series with a UV detector. The elution was performed at 170 µL/min with sulfuric acid 10 mM (pH 2.2). The column was calibrated with a mixture of formate, acetate, lactate, propionate, butyrate, and ethanol in the concentration range of 0.1 to 2 g/L.

The concentration of dissolved iron was measured by Inductively Coupled Plasma Spectroscopy (Jobin Yvon Ultima ICP).

Microbial communities were characterized at the end of some experiments. Samples of a few mL were collected and cells were concentrated by centrifugation then re-suspended in 350 mL of a lysing reagent solution. DNA was extracted using the MOBIO PowerSoil® DNA Isolation kit according to the manufacturer's instructions. 16s gene sequencing was performed on the MiSeq system to determine the microbial communities (RTLGenomics, Lubbock, USA).

The microbial settlement of stainless steel grids was observed by epifluorescence microscopy. The grids were stained with acridine orange 0.01% (A6014 Sigma) for 10 min, then washed, dried at ambient temperature and imaged with a Carl Zeiss Axiomalger M2 microscope equipped for

epifluorescence with an HBO 50W ac mercury light source and the Zeiss 09 filter (excitor HP450-490, reflector FT 10, Barrier filter LP520).

3. Results

3.1 Initial version of GLC and catalysis by stainless steel grids

Run #1 (Table 1, line 1). Four GLCs were filled with the high salinity medium inoculated with salt marsh sediments at 10% v/v. The solution was continuously fed with hydrogen and CO_2. Two of the four GLCs contained a stainless steel grid of 98 cm^2 geometric surface area. After one to two days of initial latency, formate was produced in the four reactors (Figure 2). The maximum formate production rate obtained from day 2 to day 3 reached 190 mg/L/d in the reactors packed with a stainless steel grid, which was a 50 % increase with respect to the control reactors not equipped with a grid. After 8 days, the two reactors equipped with grids had produced 417 ±57 mg/L formate, which was an increase of 48 % with respect to the controls.

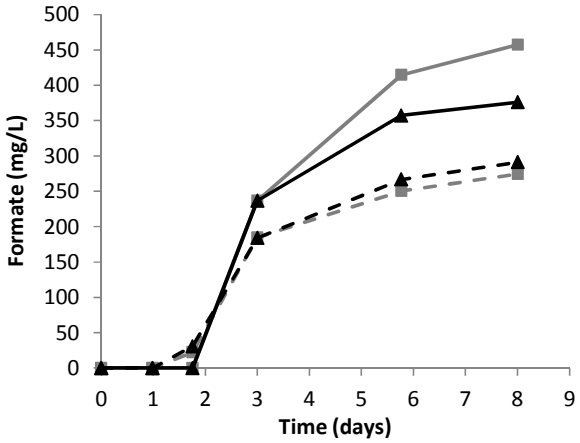

Fig 2. Formate production in high-salinity medium inoculated with salt marsh sediments (run #1). Hydrogen (3 mL/min) and CO_2 (0.6 mL/min) were bubbled through a simple pipe. Two reactors (continuous lines) were equipped with 98 cm^2 stainless steel grids.

Run #2 (Table 1, line 2). Four GLCs were implemented with the minimal medium inoculated with biological sludge at 10% v/v. Two of the four contained a stainless steel grid of 320 cm^2 geometric

surface area. Sodium 2-bromoethanesulfonate (BES) 0.5 mM was added into two of the four reactors. Acetate was produced in the four GLCs and the presence of BES (Figure 3.A) clearly improved the performance with respect to the GLCs without BES (Figure 3.B). When the solution contained BES, acetate concentration increased during the whole 17 days of the experiment and reached 1803 mg/L in the presence of the stainless steel grid packing. The maximum production rate measured between days 3 and 7 was and 289 mg/L/d, demonstrating an increase of 60 % due to the presence of the stainless steel fixed bed.

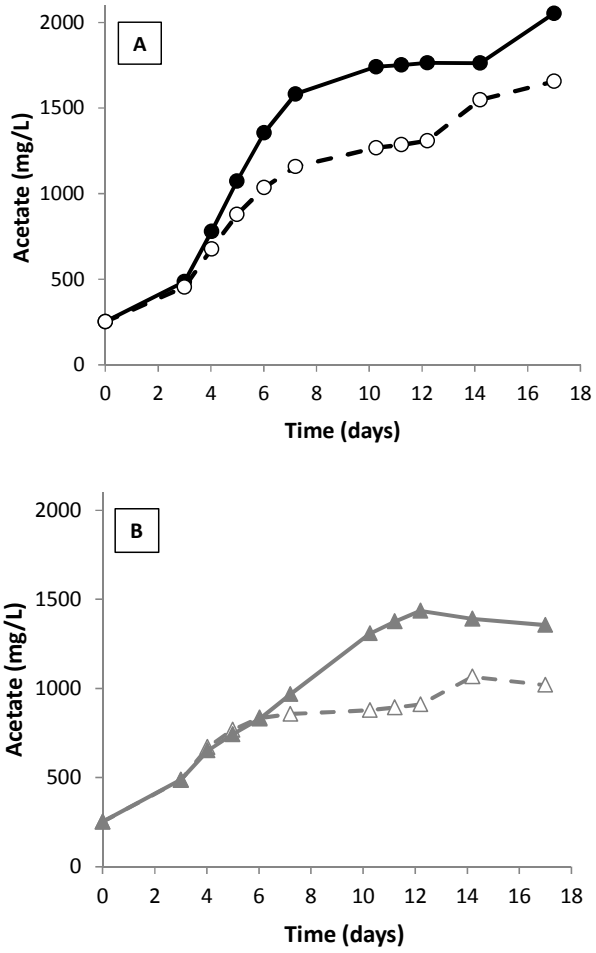

Fig 3. Acetate production in medium inoculated with biological sludge 10% v/v (run #2). Hydrogen (6 mL/min) and CO_2 (1.2 mL/min) were bubbled through a simple pipe. BES 0.5 mM was added in two reactors (A), while there was no BES in the other two (B). The initial concentration of 252 mg/L was due to the acetate content of the inoculum and the high inoculum ratio. In each case, one reactor was equipped with a 320 cm^2 stainless steel grid (continuous line), while the other was a control without a grid.

3.2 GLC with improved gas/liquid transfer and catalysis by steel wool

A comparison of the experiments performed with either salt marsh or biological sludge as the inoculum shows that the enhancing effect of the metal packing depended neither on the inoculum nor on the compound produced. The present study was continued with the biological sludge, which led to products of greater economic interest. The experimental set-up was modified so as to enhance gas-liquid mass transfer. The gas flux was provided to the solution through a porous pipe with a gas diffuser, which formed fine bubbles.

Run #3 (Table 1, line 3). The system inoculated with biological sludge at 3.3% v/v was implemented in four GLCs, two of which were equipped with a steel wool fixed bed. BES 10 mM was added into the solutions. Acetate was produced in all four GLCs and butyrate was also detected at significant concentrations. Because of the higher concentration of BES, acetate concentration increased continuously for a longer time than in the previous runs performed without BES or with a lower concentration (0.5 mM). BES inhibited the development of methanogenic species that would have converted acetate to methane [21,22].

The presence of steel wool increased the acetate production, up to concentrations of 5674 and 10671 mg/L after 41 days (Figure 4). The two GLCs filled with steel wool showed similar general behaviour but with some difference in acetate productions. The actual surface area of the steel wool that filled the two reactors may have differed from one reactor to the other and could have been a source of deviation. Nevertheless, whatever the experimental deviation, the presence of steel wool considerably enhanced acetate production, which was 2930 ±700 mg/L in both GLCs in the absence of steel wool. It should be noted that the GLC that performed the best with the steel wool fixed bed ensured a constant production rate of 265 mg/L/d for 40 days, without any intervention.

The steel wool packing also enhanced the production of butyrate. The maximum concentration obtained at the end of the experiment was 970 ±25 mg/L with the steel wool fixed bed, while butyrate appeared at 550 mg/L in only one control GLC.

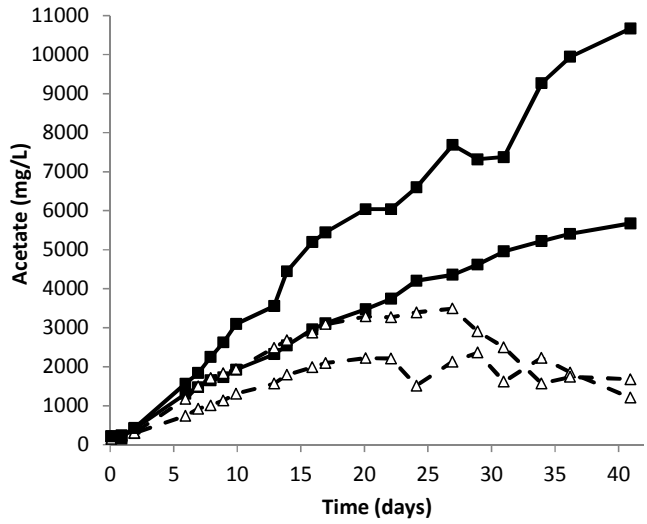

Fig 4. Acetate production in medium inoculated with biological sludge (run #3). Hydrogen (0.5 mL/min) and CO_2 (0.6 mL/min) were bubbled through a gas diffuser. BES 10 mM was added in all GLCs. Two GLCs were filled with steel wool (continuous lines) and two were not (dashed lines).

3.3 GLC with improved gas/liquid transfer and high gas flow rates, catalysis by steel wool or iron compounds.

Experiments were pursued by considerably increasing the gas flow rates to 50 mL/min for both H_2 and CO_2. The objective was to increase the gas supply to the GLCs in order to find the most efficient gas/liquid transfer that could be reached with the current experimental set-up and thus increase the productions and production rates. In the experiments described below, high gas wastage was accepted without worrying about the gas conversion ratio, in order to favour the production and production rate.

Run #4 (Table 1, line 4). Six GLCs inoculated with biological sludge (3.3 % v/v) were implemented in such gas feeding conditions. Two GLCs contained steel wool, and $FeCl_3$ at 10 mM was added into two others. All the GLCs produced acetate, butyrate and small amounts of ethanol. All showed similar general behaviour, which can be described by 3 successive phases (Figures 5 and 6): i) after initial latency of around 3 days, the first product was acetate; ii)

around day 10, the production of butyrate started while that of acetate declined; iii) production of butyrate stopped (around day 17 to 22) and its concentration stabilized close to the maximum value until the end. In this last phase, whether or not the production of acetate restarted was dependent on the operating conditions.

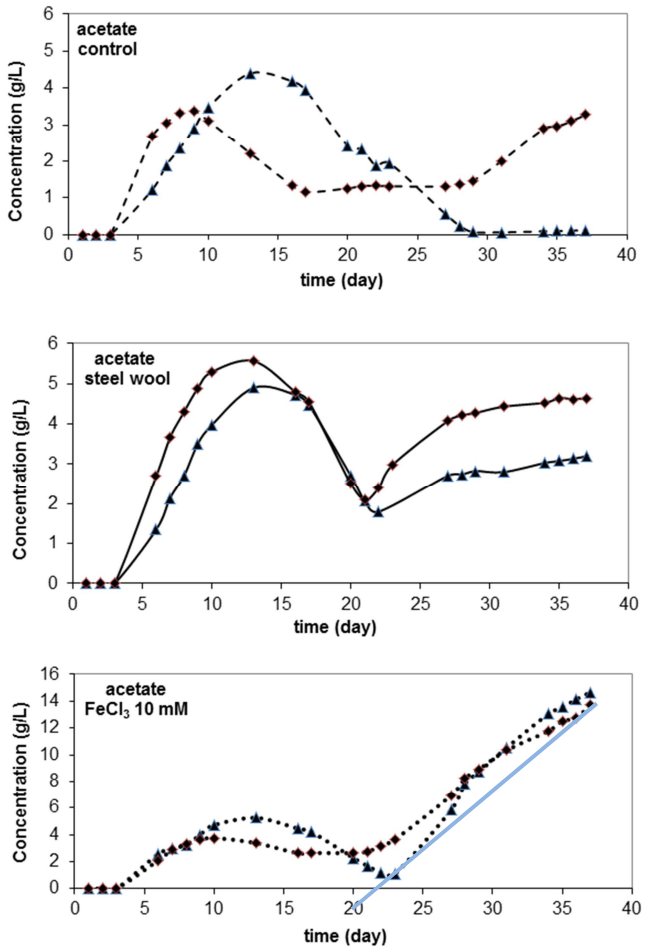

Fig 5. Acetate production in medium inoculated with biological sludge (run #4). Hydrogen and CO_2 (50 mL/min each) were bubbled through a gas diffuser. BES 10 mM was added in all reactors. Two reactors were used as controls (dashed lines), two were equipped with steel wool (continuous lines) and two contained $FeCl_3$ 10 mM (dotted lines, note that the Y-axis scale is different). The straight blue line indicates the average production rate that was maintained from around day 23 to the end.

The control GLCs and those packed with steel wool reached the maximum concentration of acetate at the end of the first phase (Figure 5). These maximum concentrations were, on average, 3890 ±510 in the controls and 5240 ±330 mg/L in the reactors with steel wool.

The GLCs that contained $FeCl_3$ 10 mM showed a considerable resumption of acetate production during the last phase so, in this case, acetate was produced at an almost continuous rate of 830 mg/L/d from day 23 to the end of the experiment at day 37 (Figure 5). Consequently, the maximum concentration of acetate of 14194 ±450 mg/L was reached at the end of the experiments. This value was considerably higher than that obtained in the other GLCs. Moreover, in the presence of $FeCl_3$ 10 mM, the duplicates showed much closer behaviour than in the other cases.

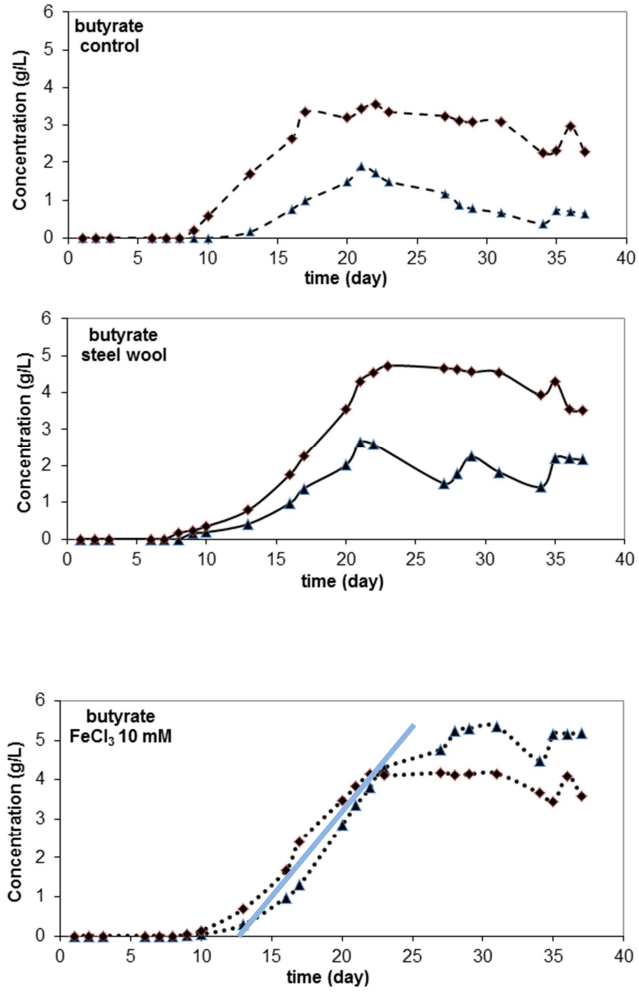

Fig 6. Butyrate production in medium inoculated with biological sludge (run #4). Hydrogen and CO_2 (50 mL/min each) were bubbled through a gas diffuser. BES 10 mM was added in all reactors. Two reactors were used as controls (dashed line), two were equipped with steel wool (continuous lines) and two contained $FeCl_3$ 10 mM (dotted lines). The blue straight line indicates the average production rate that was maintained for around 10 days.

The maximum concentrations of butyrate were 2730 ±830, 3700 ±1035, and 4725 ±630 mg/L, on average, for the control, in the presence of steel wool, and with $FeCl_3$ 10 mM, respectively. The highest concentration and the highest production rate, of 415 mg/L/d, were obtained in the presence of $FeCl_3$. In all reactors, production of ethanol was weak, with a maximum concentration of 213 ±21 mg/L in the presence of $FeCl_3$. The presence of steel wool or $FeCl_3$ enhanced the production of acetate and butyrate. $FeCl_3$ 10 mM had a greater effect, particularly because of its high impact on the last phase, after day 20.

Figure 7 gives the total amounts of carbon atoms that were present in acetate and butyrate. The curves were calculated by summing the two carbon atoms integrated into acetate and the four integrated into butyrate. This representation points out a significant, but not drastic, impact of steel wool and $FeCl_3$ 10 mM on the first phase of the process under the operating conditions used for this run. In contrast, the steel wool packing stabilized the amount of carbon atoms integrated and $FeCl_3$ 10 mM had a considerable impact by sustaining continuous integration of carbon atoms into acetate and butyrate even after 37 days of experiment.

A

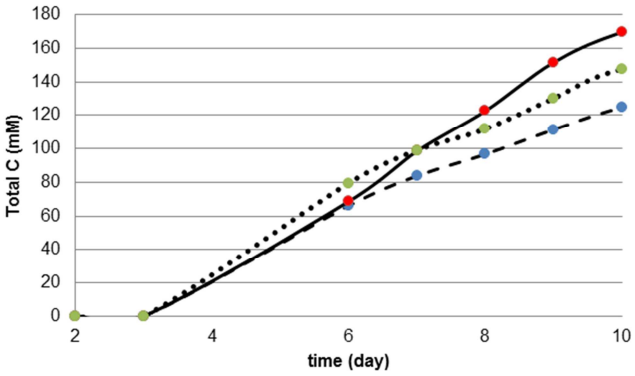

B

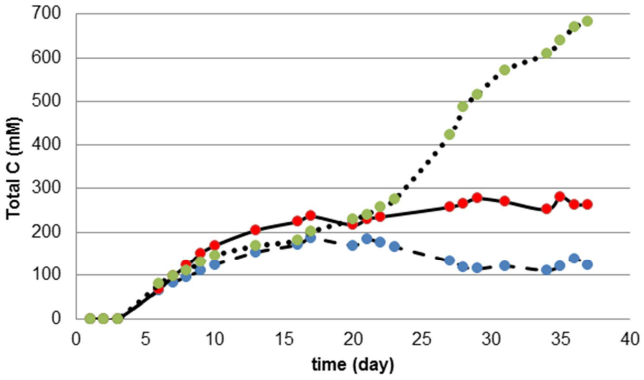

Fig 7. Carbon atoms integrated into acetate and butyrate (ethanol was neglected) during run #4 (relating to Figs. 5 and 6). Each curve averages the data from the two GLC duplicates. Control: dashed line, with steel wool: continuous lines, with $FeCl_3$ 10 mM: dotted lines A) Zoom on the starting phase; B) whole experiment duration.

Run #5 (Table 1, line 5). Finally, six GLCs inoculated with biological sludge (3.3 % v/v) were run with $FeCl_3$ 2 mM added into two GLCs and with the initial pH adjusted to 5.5 in two others. The initial pH was adjusted to 5.5 because the addition of 10 mM $FeCl_3$ in the previous run decreased the initial pH to this value, while pH was between 7.1 and 8.0 in all other GLCs. The general evolution of the concentrations with time showed the same three successive phases as those observed in the previous run (#4), except in one of the GLCs run at pH 5.5, which showed erratic behaviour. After 29 days of operation, the maximum acetate concentration (3950 ±520 mg/L) was obtained in the GLCs that contained $FeCl_3$ 2 mM and the lowest in the GLCs with pH adjusted to 5.5 (2680 ±455). The maximum butyrate concentrations were of the same order, with a maximum of 5260 ±522 mg/L. In conclusion, $FeCl_3$ at 2 mM enhanced the production of acetate and butyrate but to a lesser extent than $FeCl_3$ at 10 mM. In contrast, adjusting the initial pH to 5.5 without the presence of iron compounds in solution hampered the process.

3.4 Microbial communities

The microbial communities of the last two runs (#4 and #5) were analysed by 16S rRNA pyrosequencing (Figures 8 and 9). At the phylum level, the hydrogenation conditions considerably favoured the development of Firmicutes, which constituted less than 4% of the microbial community of the inoculum but always made up more than 20% in the GLCs (except when pH was adjusted to 5.5). Proteobacteria, which were present at a high ratio in the inoculum, were maintained at similar ratios in the control experiments and in the presence of steel wool. The presence of $FeCl_3$ enhanced the selection of Firmicutes to the detriment of Proteobacteria. This trend was particularly marked with $FeCl_3$ at 10 mM (Figure 8).

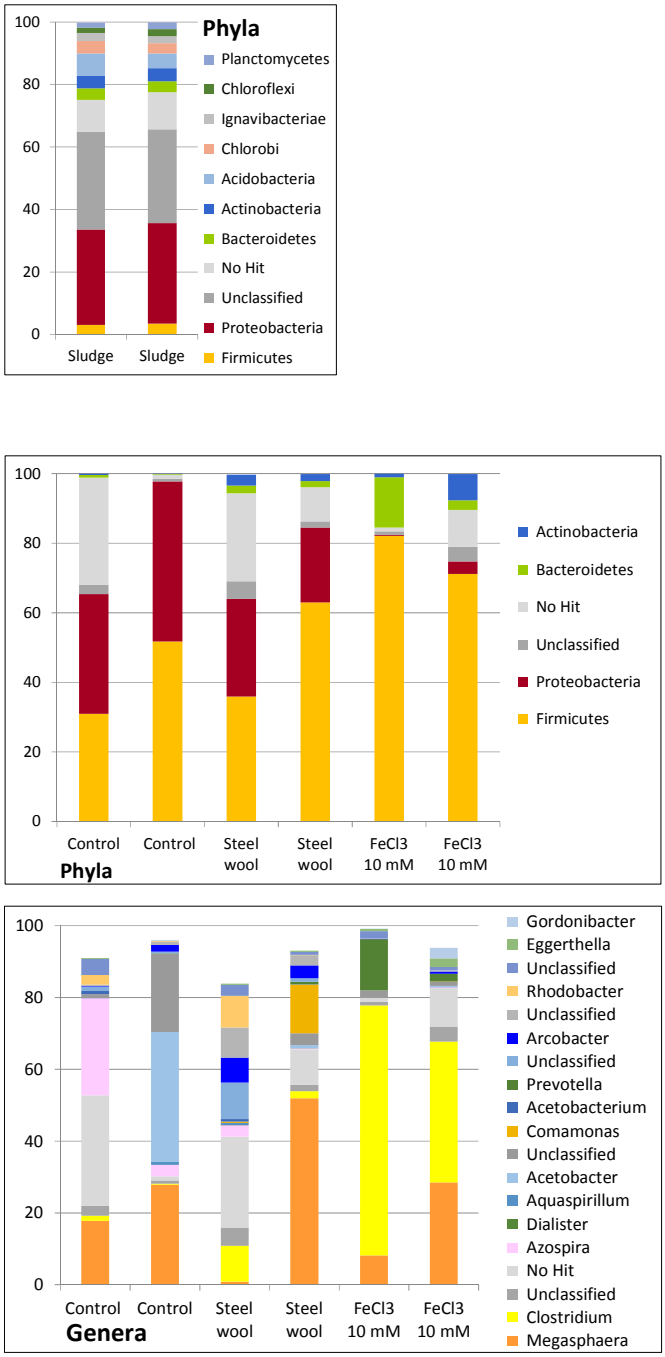

Fig 8. Major phyla and genera present in the microbial communities of the sludge used as the inoculum and of the six GLCs at the end of run #4, after 37 days of operation. Only the phyla and genera present at more than 2% in at least one sample are reported.

Analysis at the genus level showed strong selection of the two genera *Megasphaera* and *Clostridium* among Firmicutes. The control experiments and the experiments performed with the steel

wool fixed bed showed the selection of one of these two genera to the detriment of the other. In contrast, the addition of $FeCl_3$ promoted the development of *Clostridium* as the dominant genus, but without preventing the growth of *Megasphaera.* Actually, a comparison of the microbial communities obtained in the presence of $FeCl_3$ 2 mM (Figure 9) at days 27 and 41 suggests that *Clostridium* continued to grow throughout duration of the experiment, while *Megasphaera* reached a stable ratio more rapidly. Adjusting the pH to 5.5 was detrimental to these two species and promoted the alpha-Proteobacteria of genus *Acetobacter*, which was also present to a significant extent in control experiments.

Finally, at the species level, in all samples, the *Clostridium* genus was mainly represented by a single, unidentified, species that always made up more than 96% of all the *Clostridium* species detected. The *Megasphaera* genus was present with two highly dominant species, *M. sueciensis* and *M. cerevisiae*, and, to a lesser extent, *M. paucivorans*. Both the *Clostridium* and *Megasphaera* genera were represented by only a restricted number of species, which were highly dominant.

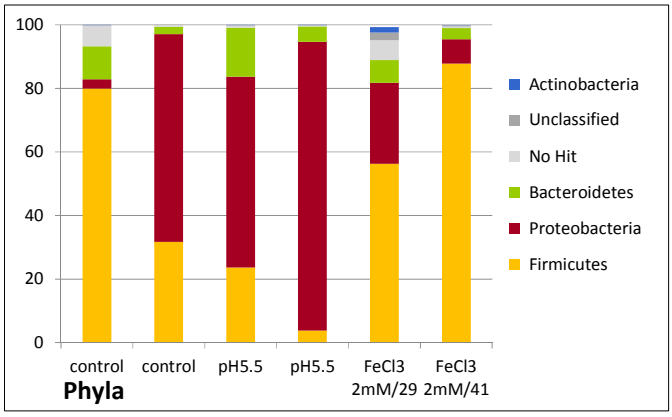

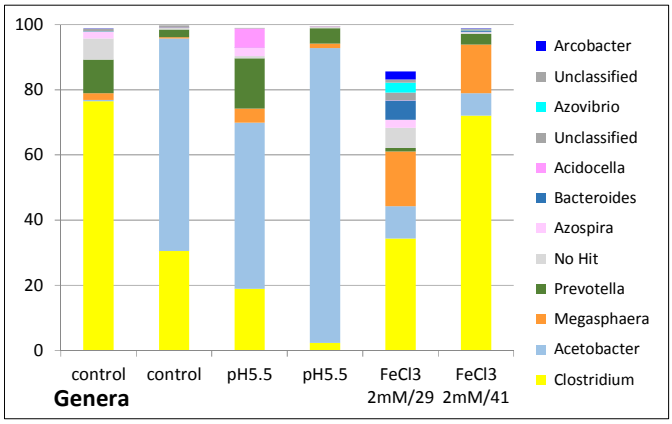

Fig 9. Major phyla and genera present in the microbial communities of the six GLCs at the end of run #5. Controls were stopped after 41 days of operation, pH 5.5 after 29 days. One GLC with $FeCl_3$ 2 mM was stopped after 29 days of operation, the other after 41 days. Only the phyla and genera present at more than 2% in at least one sample are reported.

4. Discussion

Two environmental inocula were used, one collected from salt marsh sediments and the other from the biological sludge of a water treatment plant. Both catalysed the hydrogenation of CO_2 to various products. Interestingly, the production of acetate, formate and butyrate depended on the inoculum source and on the operating conditions. For instance, with biological sludge, butyrate was detected at significant concentrations only when gas/liquid mass transfer was improved by using a porous diffuser. Adding the methanogenic inhibitor BES increased the acetate concentrations, showing that methane was probably also produced.

The preliminary tests performed with different hydrogen gas feeding configurations showed their considerable impact on the performance. When hydrogen was fed through a simple pipe, hydrogen yields were less than 1% but using a gas diffuser improved the hydrogen yields to 10.6 ±1.8 % in the presence of steel wool (run #3). These results confirmed a recent theoretical approach that modelled the microbial catalysis of CO_2 hydrogenation [23] and showed the impact of the gas supply on the conversion rate and even on the distribution of the products. The significant increase of the hydrogen yield obtained here with such a rustic improvement in the gas-liquid transfer showed the great range of improvement that was possible. Moreover, as noted above, controlling gas/liquid transfer influenced the nature of the products that were synthesized. Gas-liquid transfer should consequently be a major lever for further process improvement and control. Hydrogen yields were not an object of attention in the second part of the study (runs #4 to #6), where high gas flow rates were used in order to explore the maximum concentrations that could be reached and favour maximum production rates.

With both inoculum types, the presence of a stainless steel grid enhanced the production. This effect was significant, but fairly difficult to observe with stainless steel. For instance, the

stainless steel grids no longer had a catalytic effect when they were used for a second experiment without prior strong cleaning. Epifluorescence imaging of the grid surfaces at the end of the experiments revealed only small, and very rare, microbial settlement sites on the metal surface, showing that the catalysis did not occur via the formation of a microbial biofilm on the metal surface.

The steel wool fixed bed, which was implemented with biological sludge, led to more significant production enhancement than stainless steel did. Steel wool presented obvious signs of strong corrosion at the end of the experiments. It was thus assumed that iron released into the solution was responsible for the catalytic effect. This hypothesis was confirmed by the addition of $FeCl_3$, which enhanced both acetate and butyrate production (Table 1). With respect to the related controls, addition of $FeCl_3$ at 2 mM increased the acetate and butyrate maximum concentrations by 13 and 35 %, respectively (run #5) and $FeCl_3$ at 10 mM by 265 and 73 % (run #4). The presence of steel wool increased the maximum concentrations of both acetate and butyrate by 35% (run #4). These data are consistent with the concentration of iron of 3.0 ±0.2 mM that was measured at the end of the experiments in the GLCs equipped with steel wool. Similar measurements gave 1.8 ±0.4 and 6.8 ±1.5 mM in the GLCs to which 2 mM and 10 mM $FeCl_3$, respectively, had been added. Less than 1 µM was measured in the control GLCs. Iron was not measured in the GLCs equipped with a stainless steel fixed bed but, as no signs of corrosion were visible, it can easily be postulated that only very low concentrations of iron were released into the medium, which would explain the lower impact of the stainless steel bed and the difficulty of reproducing this effect with this material, depending on the surface state.

Salt marsh sediment led to the production of formate. In the literature, when pure cultures were used, the microbial catalysis of CO_2 conversion to formate led to 0.4 mM in 24 h with *Methanobacter formicicum* [15] and 10 mM after 2.5 days with *Desulfovibrio vulgaris* [14]. The maximal concentration of 506 mg/L (11 mM) in 22 h [13] was obtained with immobilized cells of *Alcaligenes eutrophus* under 1 atm H_2. Here, the same order of magnitude (417 ±57

mg/L) was obtained in 8 days with a multispecies culture, without optimizing the reactor design and under a hydrogen partial pressure of only 0.5 atm.

Biological sludge led mainly to the production of acetate and butyrate. Regarding acetate, the highest concentrations reported in the literature were 44.7 g/L, reached in 11 days with *Acetobacter woodii* under pressurized H_2:CO2 [24] and, recently, more than 50 g/L obtained in less than 4 days with recombinant strains [25]. The preliminary experiments described here resulted in concentrations of the same order of magnitude, up to 14.2 ±0.5 g/L, under hydrogen pressure of only 0.5 atm. These results show the great interest of environmental inocula associated with the enhancing effect of iron.

To our knowledge, only one study has used a multispecies community to produce volatile fatty acids by CO_2 hydrogenation with hydrogen gas [17]. Concentrations of 7.4 g/L acetate and 1.8 g/L butyrate were obtained after 64 days. Here, 14.2 ±0.5 g/L acetate was obtained after 37 days (run #4) and 5.2 ±0.5 g/L butyrate after 29 days (run #5). In the presence of $FeCl_3$ 10 mM, a constant production rate of acetate of 830 mg/L/d was maintained for more than 15 days. These data emphasize the great interest of adding iron into the medium to enhance production with environmental inocula.

To date, the literature does not report any similar kind of hybrid catalysis of hydrogenation reactions associating microorganisms and metallic compounds. The impact of iron compounds on microbial hydrogenation catalysed by such complex microbial communities may be the result of various mechanisms, which may be hard to unravel. Deciphering the accurate pathway(s) will now require many further dedicated studies. We offer some preliminary thoughts in this direction below.

First of all, it was observed that the addition of 10 mM $FeCl_3$ decreased the initial pH of the medium to 5.6, whereas the initial pH was between 7.1 and 8.0 in all the other GLCs. Acidification was due to the formation of iron hydroxide [26]:

$$Fe(OH)_3 \Leftrightarrow Fe^{3+} + 3\ OH^- \qquad K_s = 2.8\ 10^{-39} \qquad (2)$$

The experiments performed at pH 5.5 (run #5) in the absence of any metal catalyst (no metallic fixed bed, no iron compound) showed that acidification was not responsible for the production

enhancement observed in the presence of iron. In contrast, acidification was clearly detrimental to the production of acetate and butyrate (Table 1). The catalytic effect of iron compounds was consequently not due to the acidification they provoked. Moreover, acidification promoted the selection of Proteobacteria of the genus *Acetobacter* (Figure 9), which was mainly composed of the species *A. peroxydans*. The lower acetate production linked to the dominant presence of Proteobacteria suggests that Firmicutes were essential to reach high productions.

Two different impacts of the addition of $FeCl_3$ can consequently be distinguished: the virtuous effect of iron and the detrimental impact of pH decrease. This shapes a major avenue in the blueprint for process optimization: favouring the effect of iron while mitigating that of the associated acidification. Attempts to increase the concentration of $FeCl_3$ to 50 mM showed too drastic an acidification of the medium to pH 2.1, no longer suitable for microbial growth. On the other hand, adjusting the pH to around 8 after the addition of 10 mM $FeCl_3$ was also unsuccessful because of the formation of an intense black precipitate in the GLCs after a few days of gas feeding. The choice of optimal pH should consequently be constrained by the speciation of the metallic catalyst.

It was observed that pH decreased during the experiments in all the GLCs, from the initial value of between 7.1 and 8.0 to values ranging from 4.6 to 6.5 depending on the operating conditions. This means that pH control during operation may also be an important lever to stabilize long-term operation. The lowest pH values of 4.6 were obtained at the end of the experiments performed with 10 mM $FeCl_3$ (run #4), while the acetate production rates remained close to the maximum of 830 mg/L/d (Figure 5). When a suitable microbial community was established, the GLCs showed great robustness against significant pH drift.

Above pH 4, according to the value of the solubility product constant of iron hydroxide (K_s = 2.8 10^{-39} [26]), Fe^{3+} ions are not soluble. Most of the added iron was in the form of solid iron hydroxide or iron oxide-hydroxide and other compounds such as iron phosphate ($FePO_4.2H_2O$, Ks = 9.9 10^{-16}) and iron carbonate ($FeCO_3$, Ks = 3.1 10^{-11} [26]). Nevertheless, ICP measurements of the iron content of the solutions at the end of the experiments gave 1.8 ±0.4, 3.0 ±0.2 and 6.8 ±1.5 mM in the GLCs with 2 mM $FeCl_3$, with steel wool, and with 10 mM

$FeCl_3$, respectively. This means that a great proportion of the iron compounds was dispersed in the GLC solutions. Furthermore, the catalytic effect was linked to this concentration.

Clearly, iron concentration impacted microbial selection and the highest concentration favoured the concomitant development of the two Firmicutes genera *Clostridium* and *Megasphaera*. It is thus reasonable to postulate that iron enhances CO_2 hydrogenation by influencing microbial selection.

The presence of iron can also help the different microbial species to synthesize hydrogenases. Iron is a key component of the active sites of all types of hydrogenase [27,28] and it can be speculated that iron concentration above a given threshold may be required to trigger the synthesis of some of these enzymes. Nevertheless, the concentrations of several mM measured here are far above the values necessary for bacteria to synthesize proteins. Consequently, this hypothesis can hardly explain the higher impact of 10 mM than 2 mM $FeCl_3$. Even if the presence of iron may influence the synthesis of hydrogenases, another pathway, possibly occurring in parallel, should be evoked to explain the dependence of the catalytic effect on iron concentration.

A direct catalytic action of iron can also be speculated. Heterogeneous catalytic hydrogenation of a biocompound with hydrogen gas has already been observed with NAD^+. NAD^+ can be hydrogenated to NADH directly with hydrogen gas, in the absence of any enzyme or any other protein, when platinum is used as the catalyst [29]. Here, iron in the form of solid and dispersed oxide-hydroxide may play the conventional role of hydrogenation catalyst by adsorbing dihydrogen and thus facilitating the cleavage of the hydrogen-hydrogen bond (Figure 10, Scheme A). Hydrogenases may also be involved in this pathway, as they have been demonstrated to have the capacity to catalyse the reduction of NAD^+ to NADH by extracting hydrogen adsorbed on conductive materials [30-32].

In the field of microbial electrochemistry, outer-membrane cytochromes, which are haemproteins, and membrane-bound hydrogenases have also been postulated to be involved in electron transfer from the electrode [33-35]. Direct electron transfer from cathode to hydrogenase has also been shown in the context of enzyme electrochemistry [36]. A similar

scheme may be assumed here except that electrons did not come from an electrical circuit but from the oxidation of hydrogen (Figure 10, Scheme B).

Finally, when several species are involved, as was the case here, particularly in the presence of 10 mM $FeCl_3$, occurrence of direct interspecies electron transfer (DIET) can also be suspected. In a DIET pathway, electrons produced by a microbial species that oxidizes a first substrate are transferred directly to another species that reduces another substrate [37-39]. DIET can be speculated here from a species that was most efficient at hydrogen oxidation to a species that was most efficient at CO_2 reduction. DIET has been demonstrated to be enhanced by the mediation of conductive materials, such as magnetite nanoparticles [37] or granular activated carbon [38]. The metal-microbial catalysis described here may be the catalysis of DIET by dispersed particles of iron oxide-hydroxide (Figure 10, Scheme C).

Obviously, several of the pathways evoked above may occur in parallel and further specific studies are now required to unravel the mechanism. Experiments with pure cultures and mixed cultures of isolates should be particularly useful for this purpose.

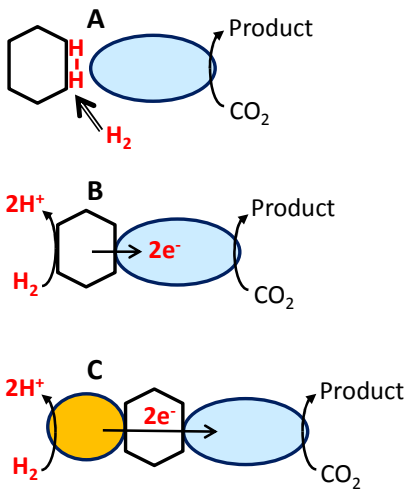

Fig 10. Scheme of possible pathways to explain the iron-microbial catalysis of CO_2 hydrogenation. A) H_2 adsorbed on iron-based particles is easier for the microbial cells to use than dissolved H_2, B) H_2 is reduced on iron-based particles, which act as cathodes by transferring electrons to the microbial cells, C) the iron-based particles catalyse direct interspecies electron transfer (DIET) from a microbial species efficient for H_2 reduction to a microbial species efficient for CO_2 reduction.

5. Perspectives

From a fundamental standpoint, the path to the identification of the right mechanism(s) of the metal-microbial catalysis described here might be a long one. In contrast, from a technological standpoint, scaling up industrial prototypes may be considerably easier and faster.

The preliminary results presented here led to high production and high production rates, particularly as far as acetate was concerned, with 830 mg/L/d sustained for more than 20 days thanks to iron catalysis. These results point out the promising potential of environmental inocula in the development of a robust process for CO_2 hydrogenation. In the context of robustness, it should be noted that using a steel wool fixed bed instead of adding $FeCl_3$ is of great interest. Firstly, for large volumes, using a fixed bed of low quality steel may be cheaper than adding $FeCl_3$. Secondly, a preliminary experiment showed that acetate and butyrate productions restarted almost immediately at maximum rates after the medium was changed in a GLC equipped with the steel wool bed (data not shown). A steel wool fixed bed should be a supplementary source of robustness of the catalytic process.

It was also shown that there is still plenty of room for improvement concerning hydrogen yields. Considering the highly efficient gas/liquid contacting processes available in the chemical industries, it is predicted that hydrogen yields will easily be increased by using the appropriate gas/liquid contactor. In this case, a membrane gas/liquid contactor, which allows maximum concentration of dissolved gas to be maintained without the formation of bubbles, should be particularly suitable [23]. Such membrane reactors have started to be proposed in order to provide biological water denitrifying reactors with H_2 and CO_2 simultaneously. In this context, H_2 was used as the electron donor and CO_2 served for pH control and as the carbon source [40,41]. Working under high gas pressure, as is commonly done for chemical hydrogenation processes, should increase the reaction efficiency even more. Finally, continuous extraction of the synthesized compounds, e.g. by electrodialysis, will also increase the production and help to maintain long-term reactor stability. All these perspectives could be envisaged in the short term because they rely only on technologies that are fully mastered at large scale in the chemical industries. For process optimization, as shown here, the balance

between pH, which should not be too low, iron speciation, and composition of the microbial community, may be the main direction to pursue in the near future.

In another context, the recent emergence of microbial electrosynthesis has brought to light many environmental inocula that catalyse the electrochemical reduction of CO_2 to various compounds [21,22,42,43]. In this framework, multispecies inocula are commonly used to form electroactive biofilms on cathode surfaces, which catalyse the electrochemical reduction of CO_2. Electrons are provided by the cathode and are assumed to be transferred to CO_2 through the microbial biofilm, which orients and catalyses the synthesis of various products. Actually, because of the low potential that must be applied to the cathode to operate at high current density, hydrogen is produced by the electrochemical reduction of water. The hydrogen produced on the cathode can then be used by the microbial cells to reduce CO_2 [44,45]. This "hydrogen route" of the electro-microbial reduction of CO_2 locally couples the production of hydrogen by water electrolysis with the microbial catalysis of CO_2 hydrogenation. Accordingly, it has recently been claimed that using gas-liquid contactors fed with hydrogen gas may be the most promising way towards the large-scale development of the microbial catalysts that have been identified in the context of electrosynthesis [18]. The fact that the species *Megasphaera sueciensis*, which was found among the dominant species in gas-liquid contactors here, has also been reported as the dominant species in electrosynthesis reactors [46] is a new, strong argument supporting this claim. The multispecies inocula successfully screened in the context of microbial electrosynthesis may consequently be excellent candidates for implementation in gas-liquid contactors fed with hydrogen gas.

Finally, beyond the examples described here, many other reactions should be screened for the possible occurrence of similar metal-microbial catalysis. For instance, the microbial conversion of syngas ($CO + H_2$), which has led to several successes even with prototypes of large volumes [47], may be a field worth investigating.

6. Conclusions

The hybrid catalysis of CO_2 hydrogenation described here associates microbial conversion with a metal catalyst. Unravelling this new catalytic pathway now constitutes a fascinating new question for researchers. Practically, concentrations of formate, butyrate and acetate reached 0.42, 5.26 and 14.19 g/L, respectively, and a production rate of acetate of 0.83 g/L/d was sustained for more than 20 days without any maintenance, showing the robustness of the process. These worthwhile results should be easy to improve by implementing equipment commonly used in the chemical industry for controlling gas/liquid transfer by following the few guidelines that have been extracted from this work.

Table 1. Operating conditions and results of the 5 experimental runs.

run #	Gas inlet	BES	Flow rates mL/min		Packing or soluble catalyst	Nb. of GLC	Maximum concentrations			Maximum production rate during starting phase	
			H_2	CO_2			Main products	mg/L	at day	mg/L/d	Duration (days)
Inoculum: salt marsh sediment											
1	Pipe	no BES	3	0.6	Control	2	Formate	283 ±12	8	126	1
					SS grid	2		417 ±57	8	190	1
Inoculum: biological sludge											
2	Pipe	no BES	6	1.2	Control	1	Acetate	816	14	105	3
					SS grid	1		1186	12	105	8
		BES 0.5 mM	6	1.2	Control	1		1406	17	180	3
					SS grid	1		1803	17	289	4
3	Porous diffuser	BES 10 mM	0.5	2	Control	2	Acetate Butyrate	2930 ±700 550	22 or 27 32	158 ±40 154	17 3
					Steel wool	2	Acetate* Acetate* Butyrate	10671 5674 970 ±25	41 41 35	265 201 82	40 27 11
4	Porous diffuser	BES 10 mM	50	50	Control	2	Acetate Butyrate Ethanol	3890 ±510 2730 ±830 163 ±18	9 or 13 21 or 22 13 or 16	580 ±85 305 ±70 -	5 7 -
					Steel wool	2	Acetate Butyrate Ethanol	5240 ±330 3700 ±1035 195 ±85	13 21 or 23 13 or 16	705 ±50 330 ±90 -	4 9 -
					$FeCl_3$ 10 mM	2	Acetate Butyrate Ethanol	14194 ±450 4725 ±630 213 ±21	37 31 or 36 13 or 16	935 ±215 415 ±30 -	8 7 -
5	Porous diffuser	BES 10 mM	50	50	Control	2	Acetate Butyrate Ethanol	3505 ±205 3900 ±40 140 ±70	29 27 13	466 ±24 303 ±20 -	5 8 to 12 -
					pH 5.5	2	Acetate Butyrate Ethanol	2680 ±455 3735 ±450 136 ±54	29 24 or 28 18	chaotic 300 ±26 -	chaotic 8 -
					$FeCl_3$ 2 mM	2	Acetate Butyrate Ethanol	3950 ±520 5260 ±522 195 ±26	29 29 15 or 17	368 ±14 360 ±45 -	4 12 -

** the duplicated GLCs gave significantly different performance and data are consequently reported separately. Some GLCs of run #5 were stopped at day 29 and others at day 41 to analyse the microbial communities at different ages. For fair comparison within this run, only the data obtained before day 29 were reported in the table.*

Acknowledgements

This work was part of the ‘‘BIORARE’’ project (ANR-10-BTBR-02), funded by the French Agence Nationale de la Recherche (ANR) and the Comité des Investissements d’Avenir. The authors thank Laure Renvoisé, Alain Huyard and Suez Environnement for supplying the biological sludge used in some of the experiments.

Conflict of interest

There are no conflicts of interest to declare.

References

1 K. Christopher and R. Dimitros, *Energ. Environ. Sci*., 2012, **5**, 6640-6651.

2 F. Zhang, P.C. Zhao, M. Niu and J. Maddy, *Int. J. Hydrogen Energ.*, 2016, **41**, 14535-14552.

3 J.Y. Zheng, X.X. Liu, P. Xu, P.F. Liu, Y.Z. Zhao and J. Yang, *Int. J. Hydrogen Energ.*, 2012, **37**, 1048-1057.

4 J.C. Lee, J.H. Kim, W.S. Chang and D. Pak, *J. Chem. Technol. Biotechnol.,* 2012, **87**, 844-877.

5 A. Bensmann, R. Hanke-Rauschenbach, R. Heyer, F. Kohrs, D. Benndorf, U. Reichl and K. Sundmacher, *Applied Energy*, 2014, **134**, 413-425.

6 I. Bassani, P.G. Kougias, L. Treu and I. Angelidaki, *Environ. Sci. Technol.*, 2015, **49**, 12585-12593 ; B. Lecker, L. Illi, A. Lemmer and H. Oechsner, *Bioresource Technol.*, 2017, **245**, 1220-1228.

7 R. Liu, X. Hao and J. Wei, *Chem. Eng. J*., 2016, **284**, 1196-1203.

8 G. Leonzio, *Chem. Eng. J*., 2016, **290**, 490-498.

9 G. Diekert and G. Wohlfarth, *Antonie Van Leeuwenhoek*, 1994, **66**, 209-221.

10 B. Schiel-Bengelsdorf and P. Dürre, *FEBS Lett.*, 2012, **586**, 2191-2198.

11 J. Mock, Y. Zheng, A. P. Mueller, S. Ly, L. Tran, S. Segovia, S. Nagaraju, M. Köpke, P. Dürre, and R.K. Thauer, *J. Bacteriol.*, 2015, **197,** 2965-2980.

12 D.D. Woods, *Biochem. J.*, 1936, **30**, 515–527.

13 A.M. Klibanov, B.N. Alberti and S.E. Zale, *Biotechnol. Bioeng.*, 1982, **24**, 25–36.

14 S.M. da Silva, J. Voordouw, C. Leitao, M. Martins, G. Voordouw and I.A.C. Pereira, *Microbiology*, 2013, **159**, 1760–1769.

15 W.-M. Wu, R.F. Hickey, M.K. Jain and J.G. Zeikus, *Arch. Microbiol.*, 1993, **159**, 57–65.

16 F. Fischer, R. Lieske and K. Winzer, *Biochem*, 1932, **245**, 2–12.

17 F. Zhang, J. Ding, Y. Zhang, M. Chen, Z.-W. Ding, M.C.M. van Loosdrecht and R.J. Zeng, *Water Res.*, 2013, **47**, 6122–6129.

18 E.M. Blanchet, F. Duquenne, Y. Rafrafi, L. Etcheverry, B. Erable and A. Bergel, *Energy Environ. Sci.*, 2015, **8**, 3731-3744.

19 R. Kleerebezem and M.C. van Loosdrecht, *Curr. Opin. Biotechnol.*, 2007, **18**, 207–212.

20 C. Dumas, R. Basséguy and A. Bergel, Electrochim. Acta 2008, **53**, 2494-2500.

21 S. Bajracharya, A. ter Heijne, X.D. Benetton, K. Vanbroekhoven, C.J.N. Buisman, D.P.B.T.B. Strik and D. Pant, *Bioresource Technol.*, 2015, **195**, 14–24.

22 M. Su, Y. Jiang and D. Li, *J. Microbiol. Biotechnol.*, 2013, **23**, 1140–1146.

23 X. Chen and B.-J. Nie, *Chem. Eng. J.*, 2016, **306**, 1092-1098.

24 M. Demler and D. Weuster-Botz, *Biotechnol. Bioeng.*, 2011, **108**, 470–474.

25 M. Straub, M. Demler, D. Weuster-Botz and P. Dürre, *J. Biotechnol.*, 2014, **178**, 67–72.

26 J.R. Rumble, ed., CRC Handbook of Chemistry and Physics, 98th Edition (Internet Version 2018), CRC Press/Taylor & Francis, Boca Raton, FL.

27 D.J. Evans and C.J. Pickett, *Chem. Soc. Rev.*, 2003, **32**, 268–275.

28 V. Artero and M. Fontecave, *Coordin. Chem. Rev.*, 2005, **249**, 1518–1535.

29 A. Bergel, H. Durliat and M. Comtat, *J. Chim. Phys.*, 1987, **84**, 593-598

30 S. DaSilva, R. Basseguy and A. Bergel, *J. Electroanal. Chem.*, 2004, **561**, 93-102.

31 K. Delecouls, P. Saint-Aguet, C. Zaborosch and A. Bergel, *J. Electroanal. Chem.*, 1999, **468**, 139-149.

32 P. Gros, C. Zaborosch, H.G. Schlegel and A. Bergel, *J. Electroanal. Chem.*, 1996, **405**, 189-195.

33 D.R. Lovley, *Energy Environ. Sci.*, 2011, **4**, 4896-4906.

34 K. Rabaey and R.A. Rozendal, *Nat. Rev. Microbiol.* 2010, **8**, 706–716.

35 M. Rosenbaum, F. Aulenta, M. Villano and L.T. Angenent, *Bioresource Technol.*, 2011, **102**, 324–333.

36 J. Cantet, A. Bergel, M. Comtat and J.-L. Seris, *J. Mol. Catal.*, 1992, **73**, 371-380.

37 S. Kato, K. Hashimoto and K. Watanabe, *Proc. Natl. Acad. Sci. U. S. A.*, 2012, **109**, 10042–10046.

38 F. Liu, A.-E. Rotaru, P.M. Shrestha, N.S. Malvankar, K.P. Nevin and D.R. Lovley, *Energy Environ. Sci.*, 2012, **5**, 8982-8989.

39 F. Aulenta, S. Rossetti, S. Amalfitano, M. Majone and V. Tandoi, *ChemSusChem*, 2013, **6**, 433–436.

40 S. Xia, C. Wang, X. Xu, Y. Tang, Z. Wang, Z. Gu and Y. Zhou, *Chem. Eng. J.*, 2015, **276**, 59-64.

41 S. Xia, X. Xu, C. Zhou, C. Wang, L. Zhou and B.E. Rittmann, *Chem. Eng. J.*, 2016, **290**, 154-160.

42 E.V. LaBelle, C.W. Marshall, J.A. Gilbert and H.D. May, *PLoS ONE*, 2014, **9**, e109935.

43 C.W. Marshall, D.E. Ross, E.B. Fichot, R.S. Norman and H.D. May, *Environ. Sci. Technol.*, 2013, **47**, 6023–6029.

44 S. Bajracharya, K. Vanbroekhoven, C.J.N. Buisman, D.P.B.T.B. Strik and D. Pant, *Faraday Discuss.*, 2017, **202**, 433-449.

45 D.R. Lovley, K.P. Nevin, *Curr. Opin. Biotechnol.*, 2013, **24**, 385–390.

46 R. Ganigue, S. Puig, P. Battle-Vilanova, M.D. Balaguer and J. Colprim, *Chem. Commun.*, 2015, **51**, 3235.

47 P. Batlle-Vilanova, R. Ganigué, S. Ramió-Pujol, L. Bañeras, G. Jiménez, M. Hidalgo, M.D. Balaguer, J. Colprim and S.Puig, *Bioelectrochemistry*, 2017, **117**, 57-64.

48 J. Daniell, M. Köpke and S.D. Simpson, *Energies*, 2012, **5**, 5372–5417.